

Thus  $E_{wc} - (\mathcal{E}_v - \alpha) = E_{wc} - E_v = \mathcal{E}_{wc} - \mathcal{E}_v = O(\alpha^2)$ , which is the required result and proves the self-consistency of our assumption,  $\mathcal{E}_{wc} - \mathcal{E}_v = O(\alpha^2)$ . [Actually the above argument does not preclude the possibility that  $|E_{wc} - E_v| < O(\alpha^2)$ .]

Next we prove that  $E_v(p)$  satisfies (20). Differentiating both sides of (29) with respect to  $p$  gives

$$\mathcal{E}_v' = g(p, \mathcal{E}_v', \mathcal{E}_v) - (\mathcal{E}_v + p^2) \times \sum \frac{2(\mathbf{k} \cdot \mathbf{p})^2 v_k^2}{p^2(1+k^2)^2} \frac{\mathcal{E}_v' - 2\mathbf{p} \cdot (\mathbf{p} - \mathbf{k})/p}{[\mathcal{E}_v - 1 - (\mathbf{p} - \mathbf{k})^2]^2} \quad (\text{A6})$$

where  $g(p, \mathcal{E}_v', 1)$  is finite. The sum on the right-hand side of (A6) diverges, however, unless  $\mathcal{E}_v' \rightarrow 0$  as  $\mathcal{E}_v \rightarrow 1$ . Since  $g(p, \mathcal{E}_v', \mathcal{E}_v)$  is linear in  $\mathcal{E}_v'$ , no solution of (A6) exists when  $|\mathcal{E}_v'| \rightarrow \infty$ , hence  $\mathcal{E}_v' = E_v' \rightarrow 0$  as  $\mathcal{E}_v \rightarrow 1$ , which is the required result.

We have remarked earlier that to order  $\alpha^2$ ,  $c_k$  is given by an expression of the form

$$c_k = j(\mathbf{k}, \mathbf{p})_c / [E_{wc} - \mathcal{G}(\mathbf{k}, \mathbf{p}) - 1 - (\mathbf{p} - \mathbf{k})^2], \quad (\text{A7})$$

where

$$\lim_{\mathcal{E}_{wc} \rightarrow 1} \mathcal{G}(\mathbf{p}, \mathbf{p}) = E_{wc}(0)$$

and  $E_{wc}(0)$  is the exact ground state to order  $\alpha^2$ . This means that to order  $\alpha^2$

$$E_{wc} - p^2 = \sum j(\mathbf{k}, \mathbf{p}) / [E_{wc} - \mathcal{G}(\mathbf{k}, \mathbf{p}) - 1 - (\mathbf{p} - \mathbf{k})^2]. \quad (\text{A8})$$

Since for weak coupling  $j(\mathbf{p}, \mathbf{p}) \neq 0$  when  $\mathcal{E}_{wc}(p) = 1$  the above argument proving that  $\mathcal{E}_v'(p) = 0$  when  $\mathcal{E}_v = 1$  can be applied to (A8) to prove that  $\mathcal{E}_{wc}'(p) = 0$  when  $\mathcal{E}_{wc} = 1$  to order  $\alpha^2$ . It is tempting to think that (A8) is valid to arbitrarily high order in perturbation theory. The main problem is to prove that  $\mathcal{G}(\mathbf{p}_c, \mathbf{p}_c)$  is equal to the ground-state polaron energy to infinite order in Wigner-Brillouin perturbation theory and that  $j(\mathbf{p}_c, \mathbf{p}_c) \neq 0$ . In this way the conjecture of Schultz *et al.* could presumably be established for all  $\alpha$  for which the Wigner-Brillouin ground-state perturbation theory converges.

## Nonlinear Galvanomagnetic Effect of *n*-Type InSb in the Quantum Limit

KIICHI F. KOMATSUBARA AND EIZABURO YAMADA

*Hitachi Central Research Laboratory, Kokubunji, Tokyo, Japan*

(Received 4 October 1965; revised manuscript received 30 November 1965)

Nonlinear galvanomagnetic effects in *n*-type InSb in the quantum limit were studied, using uncompensated samples with an impurity concentration of  $1.1 \times 10^{14}$  atoms/cm<sup>3</sup>. The nonlinear characteristics observed at 1.5°K and in transverse magnetic fields above 2 kG are caused by the heating of conduction electrons under conditions where the frequency of collisions with ionized impurities is much larger than that with acoustic phonons. The ratio of the frequency of collision with ionized impurities to that with acoustic phonons is about  $4 \times 10^4$ . The carrier heating begins to have a large effect near the electric field  $E_1$ , which is given by  $(sB/c)(\tau_{im}/\tau_{ph})^{1/2}$ . The value of  $E_1$  at 10 kG is about 0.1 V/cm. The electric field  $E_2$  which raises the electron energy so that quantum conditions are not satisfied is proportional to  $0.11B^{1/2}\alpha^{1/2}E_1$  where  $\alpha$  is about 4. Observations on compensated samples, where freeze-out effects are seen, and on samples of greater impurity concentration, where Shubnikov-de Haas oscillations are seen, are also discussed.

### INTRODUCTION

IT is possible to obtain the quantum-limit conditions,  $\omega_c \tau \gg 1$ ,  $\hbar \omega_c > E_f$ ,  $\hbar \omega_c > kT$ , in samples of the purest *n*-type InSb at sufficiently low temperature, in the range of easily achievable static magnetic fields. This is in part due to the small effective electron mass and the corresponding large mobility.<sup>1</sup> In such samples, the scattering by the ionized impurities is a dominant factor in the transport phenomena, because of the comparatively large de Broglie wavelength of the electrons. Kazarinov and Skovob<sup>2</sup> have shown that a nonlinear galvanomagnetic effect of a quantum-mechanical nature

is expected in these samples, when strong crossed electric and magnetic fields are applied.

However, in addition to the quantum effects, there are effects caused by the freeze-out of the conduction electrons in strong magnetic fields. The donor impurity levels of InSb split off from the conduction band because of the shrinkage of the donor wave functions when a strong magnetic field is present. As a result, carriers are likely to fall into the split-off impurity band with its lower mobility. When a strong electric field is applied in samples under these circumstances, impact ionization of these carriers from the split-off band to the conduction band is observed.

<sup>1</sup> E. N. Adams and R. W. Keyes, in *Progress in Semiconductors*, edited by A. F. Gibson (Heywood and Company, Ltd., London, 1962), Vol. 6, p. 126.

<sup>2</sup> R. F. Kazarinov and V. G. Skovob, Zh. Eksperim i Teor. Fiz.

42, 1047 (1962) [English transl.: Soviet Phys.—JETP 15, 726 (1962)].

In several previous studies of the nonlinear galvanomagnetic behavior of *n*-type InSb at liquid-helium temperature,<sup>3-5</sup> there are discussions of the situation when freeze-out and impact ionization play dominant roles. Nonlinear effects caused by carrier heating have been studied experimentally by Putley.<sup>5</sup> He pointed out that carrier heating also occurs in the presence of a weak magnetic field. However, he discussed his results on the basis of a classical warm-electron theory.

We have measured the galvanomagnetic effects in *n*-type InSb samples with impurity concentrations of  $10^{14} \sim 10^{15}$  atoms/cm<sup>3</sup>, with and without compensation, at liquid-helium temperatures in transverse magnetic fields up to 13.5 kG. In uncompensated samples with impurity concentration of  $1.1 \times 10^{14}$  atoms/cm<sup>3</sup>, we have observed nonlinear galvanomagnetic phenomena which depend on the quantum-limit conditions, and are thus different from those caused by impact ionization. We interpret our experimental results using the theory of the conductivity in the quantum limit.

### EXPERIMENTAL RESULTS

We used essentially uncompensated samples of *n*-type InSb (sample code C2-143) with an impurity concentration of  $1.1 \times 10^{14}$  atoms/cm<sup>3</sup>, a compensated sample

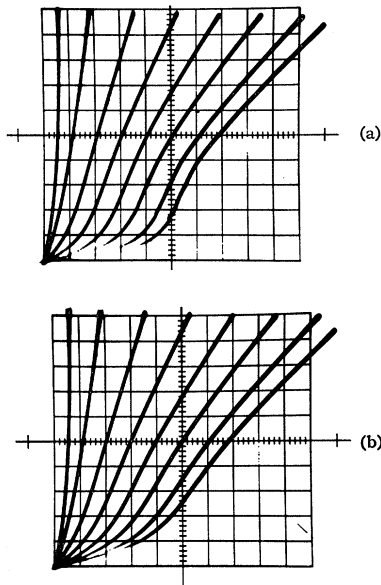


FIG. 1. Current versus voltage curves of an uncompensated sample with  $1.1 \times 10^{14}$  atoms/cm<sup>3</sup> (C2-143-Z2). The curves correspond to 0, 2, 4, 6, 8, 10, 12, and 13.5 kG, from left to right, respectively. The divisions on the vertical and horizontal scales are 1 mA and 0.1 V, respectively. The temperature was 1.5°K for (a) and 4.2°K for (b).

<sup>3</sup> R. J. Sladek, *J. Phys. Chem. Solids* **5**, 157 (1958).

<sup>4</sup> R. J. Phelan, Jr. and W. F. Love, *Phys. Rev.* **133**, A1134 (1964).

<sup>5</sup> E. H. Putley, in *Physics of Semiconductors; Proceedings of the Seventh International Conference, Paris, 1964* (Dunod Cie., Paris, 1964), p. 443.

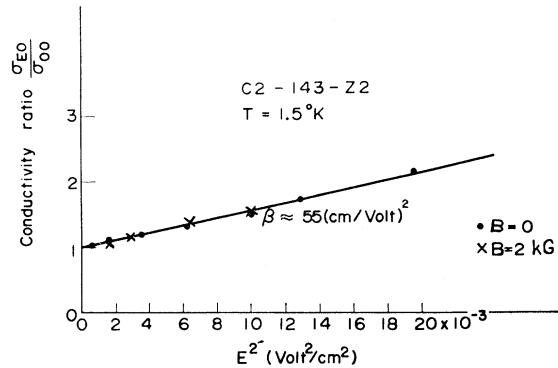


FIG. 2. Relative conductivity versus the square of the electric field for the sample C2-143-Z2 at 0 and 2 kG and at 1.5°K.

(C2-281) with an impurity concentration of  $2 \times 10^{14}$  atoms/cm<sup>3</sup>, and Te-doped *n*-type InSb samples (C2-323) with an impurity concentration of  $1.4 \times 10^{15}$  atoms/cm<sup>3</sup>. The samples were cut in bars 0.8 mm  $\times$  1.0 mm  $\times$  7.0 mm, and the low-frequency pulsed electric field was applied along the long side of the bars (the  $\langle 111 \rangle$  direction), while the magnetic field was applied transverse to the electric field (the  $\langle 110 \rangle$  direction).

When the electric field was applied to the samples C2-143, nonlinear characteristics which are different from those caused by impact ionization were observed at temperatures below 7°K and in transverse magnetic fields above 2 kG. Figure 1(a) shows the observed relations between the current, *I*, and the electric field, *E*, at 1.5°K in the sample C2-143-Z2. As can be seen in this figure, the curve without magnetic field (at the far left) rises more rapidly than it extends linearly, because of the heating of the electrons and the large contribution of ionized impurity scattering. As seen in Fig. 2, the coefficient,  $\beta$ , in the mobility relation,  $\mu = \mu_0 (1 + \beta E^2)$ , was about  $55 \text{ cm}^2 \text{V}^{-2}$ .

Figure 1(b) shows the *I*-versus-*E* curves at 4.2°K. The tendency of the curves does not change in the region between 4.2 and 1.5°K, indicating that the samples are degenerate throughout this range.

In compensated samples, effects due to freeze-out are more predominant than the quantum-limit effects, as shown in Fig. 3 for sample C2-281-Z1. The tendencies of the curves are very different at 4.2 and 1.5°K. This behavior leads us to conclude that degeneracy temperature in this sample may lie below 4.2°K.

These kinds of nonlinear behavior are not observed in uncompensated samples containing impurity concentrations greater than  $5 \times 10^{14}$  atoms/cm<sup>3</sup>. An example of their behavior is shown in Fig. 4, which presents the *I*-versus-*E* curves for the sample C2-323-Z3, which contains an impurity density of  $1.4 \times 10^{15}$  atoms/cm<sup>3</sup>.

Plots of the ratio  $\rho_T/\rho_{00}$  as a function of *E* are presented in Figs. 5, 6, and 7, which correspond to Figs. 1, 3 and 4, respectively.  $\rho_T$  is the resistivity in the transverse magnetic field and  $\rho_{00}$  is the Ohmic resistivity without magnetic field.

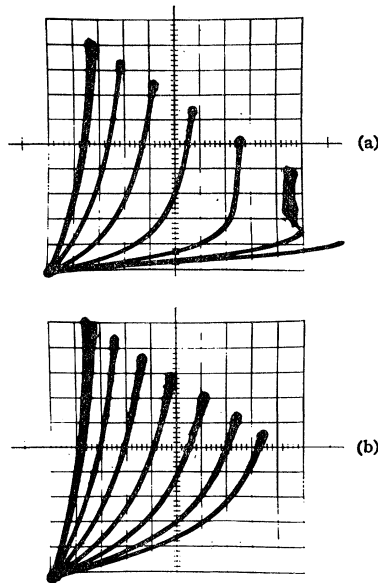


FIG. 3. The current-versus-voltage curves in the compensated sample with  $2 \times 10^{14}$  atoms/cm<sup>3</sup> (C2-281-Z1). The curves correspond to 0, 2, 4, 6, 8, 10, and 12 kG from left to right, respectively. The divisions on the vertical and horizontal scales are 0.05 mA and 0.2 V, respectively. The temperature was 1.5°K for (a) and 4.2°K for (b).

### DISCUSSION OF THE RESULTS

In order to clarify the conditions for the observation of various effects on the galvanomagnetic properties, we represent the  $B$  and  $T$  dependence of several quantum conditions in Fig. 8.<sup>1</sup> Plotted are curves tracing the condition  $\omega_c \tau = 1$  and the magnetic field at which carrier freeze-out sets in, for both uncompensated and compensated samples with impurity concentrations of  $10^{14}$  and  $10^{15}$  atoms/cm<sup>3</sup>. Also plotted is the quantum condition  $\hbar \omega_c = kT$ . We see that the quantum-limit conditions  $\hbar \omega_c > E_f$ ,  $\hbar \omega_c > kT$ ,  $\omega_c \tau \gg 1$  can be easily achieved in samples with an impurity concentration of  $10^{14}$  atoms/cm<sup>3</sup> at temperatures below 7°K and in magnetic fields above 2 kG. In highly compensated samples with the same net impurity concentration, a much stronger magnetic field is necessary to satisfy the condition  $\omega_c \tau \gg 1$ , even though  $\hbar \omega_c > E_f > kT$  at the same temperature and fields. Therefore quantum-limit effects are difficult to observe because they are confused by the freeze-out effects, which set in at the strong magnetic fields.

Samples with  $10^{15}$  atoms/cm<sup>3</sup> show an oscillatory magnetoresistance under quantum conditions at relatively weak magnetic fields. The quantum-limit condition in these samples may then appear in the strong-magnetic-field region. However, their quantum-limit behavior may also be confused by freeze-out effects.

In  $n$ -type InSb with an impurity concentration of  $10^{14}$  atoms/cm<sup>3</sup>, the ionized-impurity scattering is dominant at low temperatures, as seen in Fig. 2. The value 55

cm<sup>2</sup>V<sup>-2</sup> for  $\beta$  is very large compared with the cases<sup>6</sup> of germanium and silicon. It is not clear that the usual Born-approximation treatment is applicable in our case. However, we used the Born approximation and estimated from this value of  $\beta$  that the ratio  $\tau_{ph}/\tau_{im}$  is about  $4 \times 10^4$ , where  $\tau_{ph}$  and  $\tau_{im}$  are the collision times for acoustic and ionized-impurity scattering, respectively.

The condition  $\omega_c \tau \gg 1$ , where  $\tau^{-1} = \tau_{ph}^{-1} + \tau_{im}^{-1}$ , is approximately satisfied throughout the measured range of magnetic fields in the case of samples C2-143. Therefore, the component of current along the direction of the applied electric field is produced by jumps of cyclotron orbit centers due to collisions. The power gain of the carriers from the electric field is proportional to  $\tau^{-1}$ , while the energy loss transferred to the lattice is proportional to  $\tau_{ph}^{-1}$ .

Kazarinov and Skobov<sup>2</sup> have shown that appreciable heating of carriers occurs under these conditions and that the electron temperature  $T_e$  can be expressed in the following form:

$$T_e = T \left[ 1 + \frac{1}{2} (cE/sB)^2 (1 + \tau_{ph}/\tau_{im}) \right], \quad (1)$$

where  $c$  is the velocity of light and  $s$  is the velocity of sound.

For samples containing  $1.1 \times 10^{14}$  atoms/cm<sup>3</sup> at 1.5°K, the relation  $\hbar \omega_c > E_f > kT$ , which is the condition for the quantum limit and degeneracy, can be satisfied for magnetic fields larger than 2 kG. When the applied

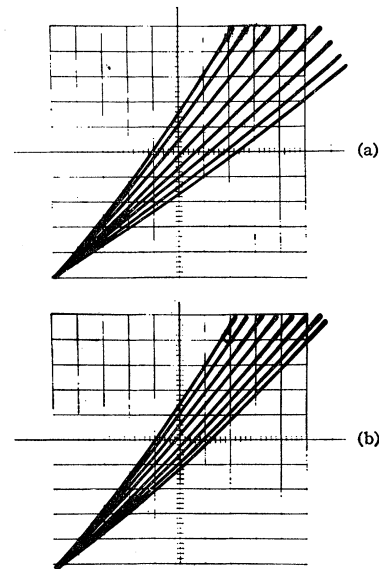


FIG. 4. The current-versus-voltage curves in the sample with  $1.4 \times 10^{15}$  atoms/cm<sup>3</sup> (C2-323-Z3). The curves correspond to 0, 2, 4, 6, 8, 10, 12, and 13.5 kG from left to right, respectively. The divisions on the vertical and horizontal scales are 5 mA and 0.1 V, respectively. The temperature was 1.5°K for (a) and 4.2°K for (b).

<sup>6</sup> J. B. Gunn, *Progress in Semiconductors*, edited by A. F. Gibson (Heywood and Company, Ltd., London, 1957), p. 213.

FIG. 5.  $\rho_T/\rho_{00}$  versus electric field for conditions corresponding to those of Fig. 1(a).  $\rho_{00}$  is the resistivity at  $B=0$  and  $E \rightarrow 0$ .

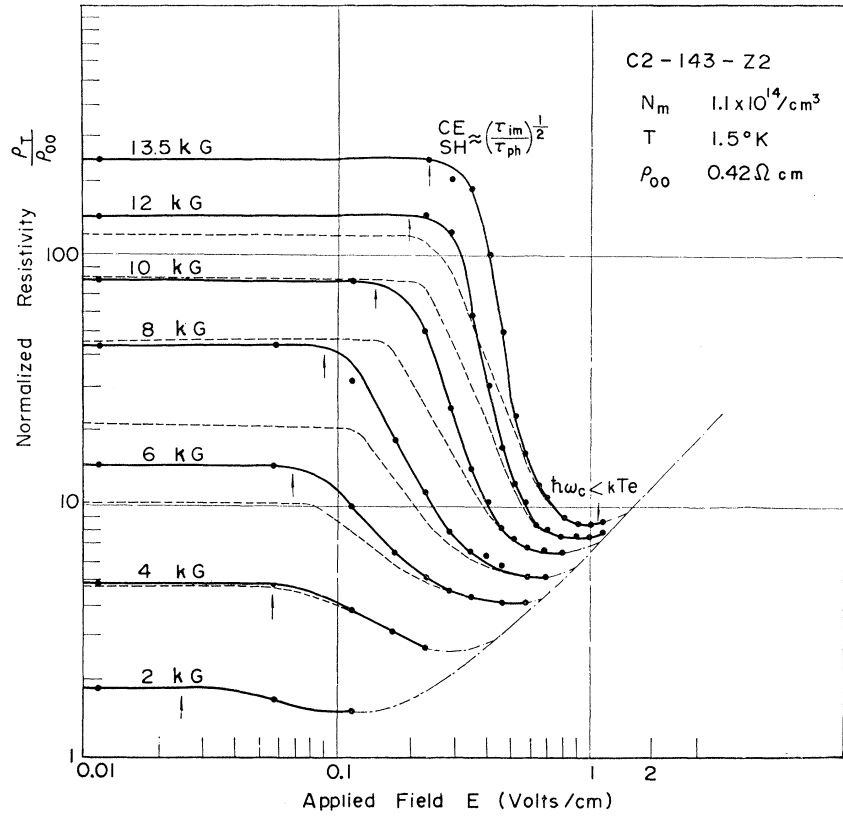
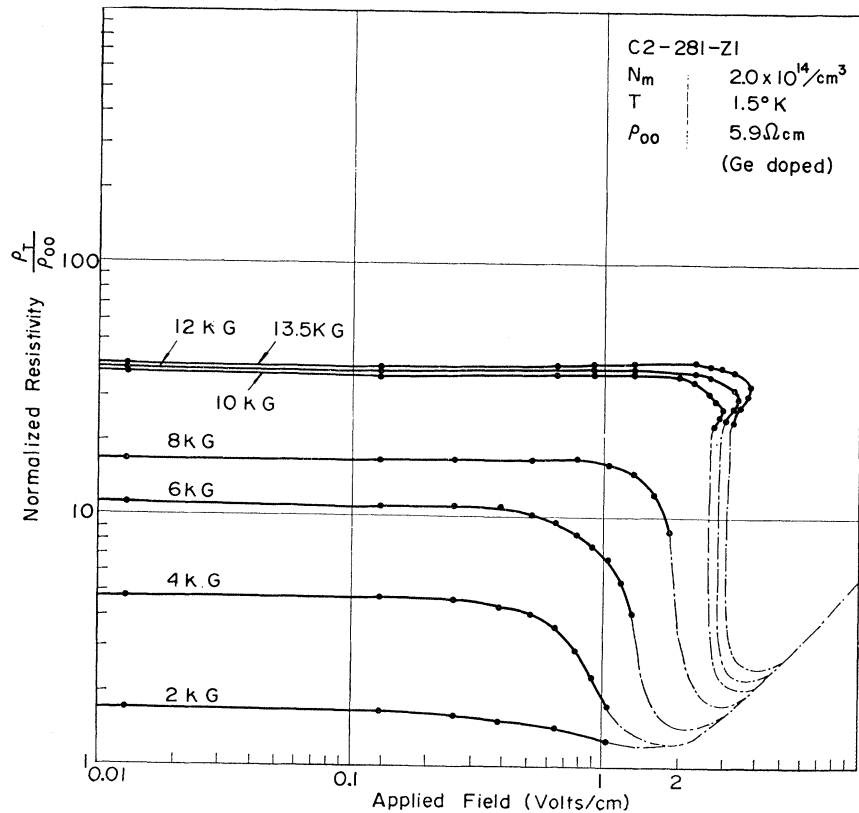


FIG. 6.  $\rho_T/\rho_{00}$  versus electric field for the compensated sample (C2-281-Z1) under conditions corresponding to those of Fig. 3(a). Impact ionization is seen in the higher-magnetic-field curves.



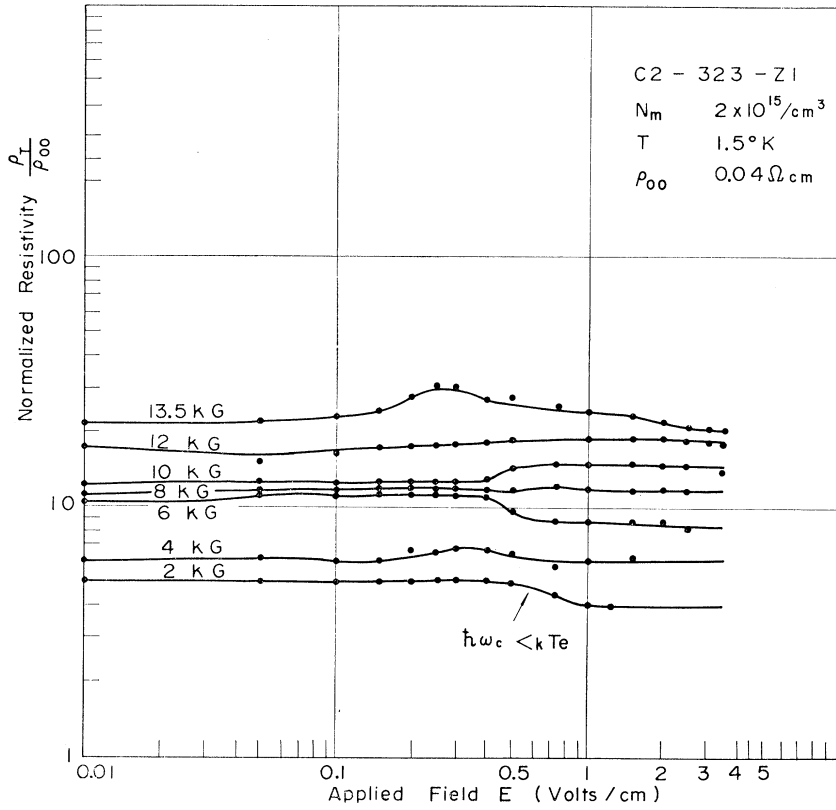


FIG. 7.  $\rho_T/\rho_{00}$  versus electric field for the sample with  $10^{15}$  atoms/cm<sup>3</sup> (C2-323-Z3) under conditions corresponding to Fig. 4(a).

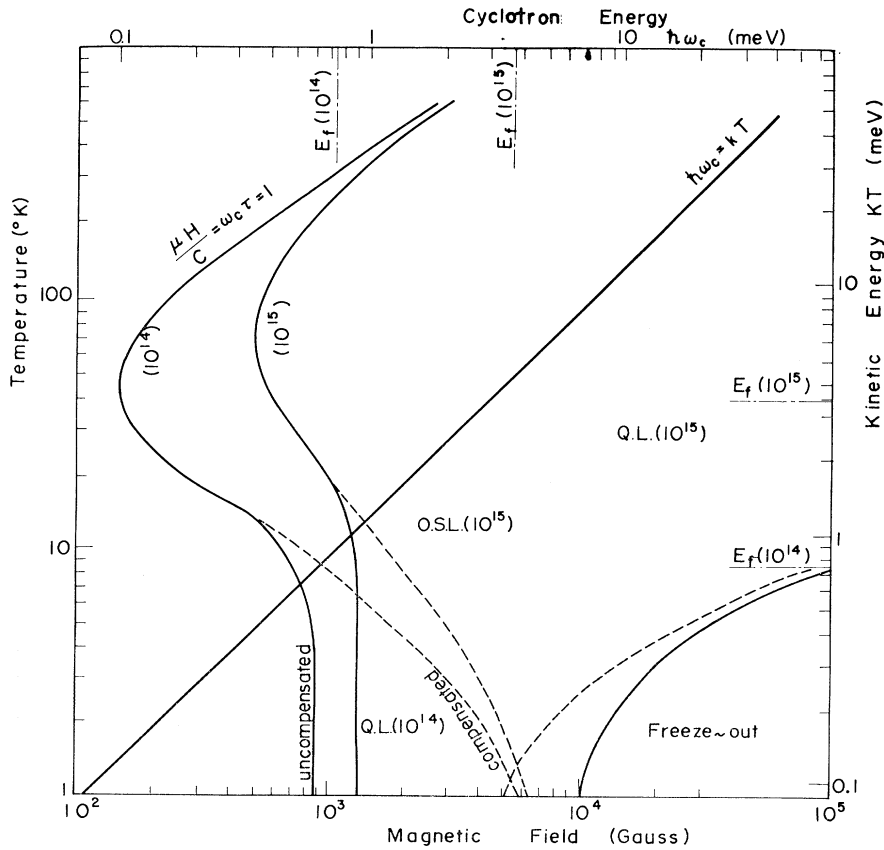


FIG. 8. Plot of conditions determining the quantum regions for samples of InSb with  $N=10^{14}$  and  $10^{15}$  atoms/cm<sup>3</sup>. The vertical scale is marked with absolute temperature on the left side and the equivalent energy ( $kT$ ) on the right side. The horizontal scale is marked in gauss on the bottom and in the energy equivalent ( $\hbar\omega_c$ ) on the top. Quantum-limit effects can be observed in the region QL; oscillatory effects can be seen in the region OSL.

electric field exceeds the value

$$E_1 \approx sB/c(\tau_{im}/\tau_{ph})^{1/2}, \quad (2)$$

$T_e$  rises appreciably above the lattice temperature and the electrons become nondegenerate. With further increase of electric field,  $kT_e$  exceeds  $\hbar\omega_c$ . Consequently, the effect of quantization of the orbit disappears and a classical treatment should be valid in this high-electric-field region. The electric field at which  $kT_e = \hbar\omega_c$  is

$$E_2 \approx E_1 \alpha^{1/2} (\hbar\omega_c/kT)^{1/2} = 0.11 B^{1/2} \alpha^{1/2} E_1, \quad (3)$$

where  $m^* = 0.014m_0$ ,  $T = 1.5^\circ\text{K}$  and  $\alpha = (\tau_{im}/\tau_{ph})_{\text{high}E} / (\tau_{im}/\tau_{ph})_{\text{low}E}$ .

In Fig. 5, the resistivity ratio  $\rho_T/\rho_{00}$  is plotted as a function of the electric field, with  $\rho_{00} = 0.42 \Omega\text{-cm}$ , the resistivity at  $B=0$  and  $E \rightarrow 0$ . We observed that the Hall coefficient in the Ohmic region of the  $I$ -versus- $E$  curves increased with magnetic field for magnetic fields larger than 6 kG. This indicates that some fraction of the carriers are freezing out. For electric fields larger than  $E_1$ , the Hall coefficient decreases with electric field until it reaches its exhaustion value, that is, the value for low magnetic field. Therefore, we see that there are two reasons for the increase of  $\rho_T$  with  $B$  in the Ohmic region, namely, the magnetoresistance and the carrier freeze out. When we correct for the effect of carrier freeze-out using the Hall coefficient data, we obtain the dashed curves.<sup>7</sup> A value of 4 for  $\alpha$  is obtained from these dashed curves.

As can be seen from Fig. 9, the corrected values of  $\rho_T$  when  $E \rightarrow 0$  follow the relation  $\rho_T \sim B^3 T^0$ . This relation agrees with the prediction of Adams and Holstein<sup>8</sup> for the quantum-limit transverse magnetoresistance of degenerate semiconductors in which ionized-impurity scattering is predominant. When the electric field exceeds  $E_1$  and nondegenerate statistics become applicable, a relation  $\rho_T \sim B^0 T_e^{-3/2}$  holds for ionized-impurity scattering.

Substituting Eq. 1 for  $T_e$ , we have the relation in the form  $\rho_T \sim B^3 E^{-3}$  for the nonlinear region. In Fig. 5, the dashed curves near 10 kG follow this dependence on  $B$  and  $E$ . The values of  $E_1$  shown by the arrows in Fig. 5 are proportional to  $B$ . Assuming that  $\tau_{im}/\tau_{ph}$  does not depend on  $B$ , we calculate the sound velocity in InSb

<sup>7</sup> We have assumed that the mobility of electrons in the freeze-out state is negligible. This is valid (see Ref. 3) for magnetic fields higher than 10 kG.

<sup>8</sup> E. N. Adams and T. D. Holstein, J. Phys. Chem. Solids **10**, 254 (1959).

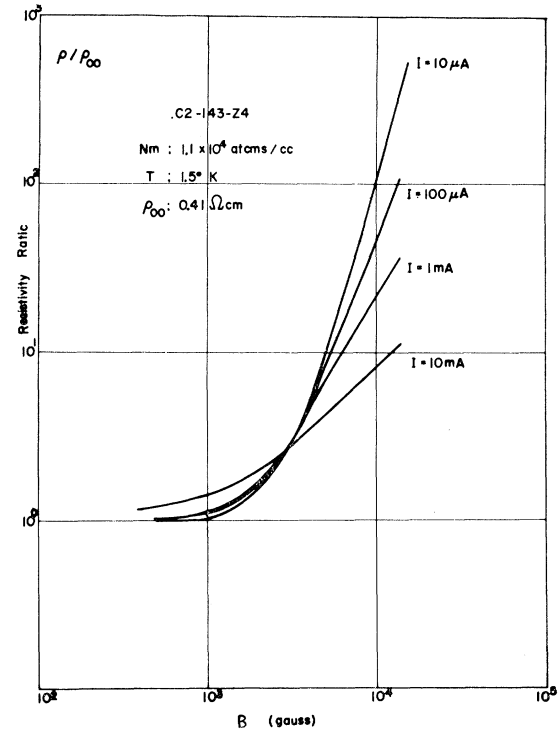


FIG. 9. The relation between resistivity and transverse magnetic field in the sample C2-143-Z4 with the current as a parameter. The  $B^3$  dependence of the resistivity can be seen in the low current (Ohmic) region.

to be  $2 \times 10^5$  cm/sec, which is in good agreement with the known value of  $3.8 \times 10^5$  cm/sec.

This type of nonlinear behavior is observed only in uncompensated samples containing an impurity density of about  $10^{14}$  atoms/cm<sup>3</sup>. The change of  $\rho_T/\rho_{00}$  with electric fields of a compensated sample is shown in Fig. 6 for comparison.

The magnetoresistance  $\rho_T/\rho_{00}$  as a function of  $E$  for a sample containing an impurity density of  $2 \times 10^{15}$  atoms/cm<sup>3</sup> is shown in Fig. 7. The magnetoresistance at weak electric fields shows Shubnikov-de Haas oscillations with a period of  $3.6 \times 10^{-4} \text{ G}^{-1}$ . This oscillatory behavior disappears when the electric field exceeds  $E_2$  (where  $\hbar\omega_c < kT_e$ ) as a result of the broadening of the Landau levels.

#### ACKNOWLEDGMENTS

The authors wish to thank Dr. M. Glicksman and Professor Y. Uemura for valuable discussions, and N. Takasugi for assistance in the experiments.